Reliability Engineering and System Safety 260 (2025) 111040

Contents lists available at ScienceDirect

Reliability Engineering and System Safety

journal homepage: www.elsevier.com/locate/ress

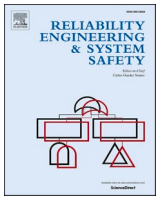

Resilience modeling and evaluation of multi-state system with common bus performance sharing under dynamic reconfiguration

Gengshuo Hu, Xing Pan, Jian Jiao *

School of Reliability and Systems Engineering, Beihang University, Beijing 100191, China

ARTICLE INFO

Keywords:
Resilience
Multi-state system
Performance sharing
Dynamic reconfiguration
Universal generating function

ABSTRACT

Multi-state systems with common bus performance sharing (MSS-CBPS) are widely applied in the industry, including integrated modular avionics (IMA) and computing systems. In the presence of uncertain disturbances, dynamic reconfiguration can enhance the ability to manage these uncertainties effectively. Resilience can significantly describe the ability of systems to recover from disturbances. However, effective methods have not fully been proposed to model and evaluate their resilience against disturbances. To address this issue, this paper introduces a novel resilience model based on the structure and characteristics of the MSS-CBPS, incorporating dynamic reconfiguration strategies and performance allocation sequences. Furthermore, the model comprehensively evaluates system resilience through resistance, response, and recovery resilience metrics. Based on the novel resilience model, an algorithm based on the universal generating function (UGF) is developed to evaluate system resilience accurately under different dynamic reconfiguration strategies. Finally, the model and algorithm are applied to an integrated task processing system in a helicopter to demonstrate their feasibility by analyzing resilience tendencies under different dynamic reconfiguration strategies. The results also provide valuable insights for designing integrated task processing systems.

1. Introduction

With the rapid development of industrial and scientific technologies, industrial systems such as power supply systems [1], transmission systems [2], and computing systems [3] have become increasingly complex. The units of such systems typically have multiple states and can share resource through a common bus. In other words, the resource surplus of some units can be shared with the unit with resource deficiency via a common bus [4]. For this type of system, resource sharing among units increases system complexity. It also increases the risk when the system is disturbed. System resilience, which refers to the ability to maintain performance by reallocating resources in the face of disturbances, provides a new approach to meet the challenges. Enhancing the system resilience can effectively improve the capacity to manage risks. Although resilience has become a prominent topic in various fields, research on resilience of multi-state system with common bus performance sharing remains largely unexplored [5]. Moreover, traditional resilience assessment models and methods may encounter challenges in accurately capturing the dependencies between units and performance reallocation mechanisms, which are essential for analyzing the system resilience. Therefore, these models and methods cannot analyze the resilience of multi-state system with common bus performance sharing accurately. It is crucial to conduct research on resilience modeling and evaluation for this type of system.

For the multi-state system with common bus performance sharing (MSS-CBPS), some research effort has been devoted toward the modeling of MSS-CBPS, such as the model for the system consisting of main and backup units, where the performance surplus can be transferred from backup units to main units [6] as well as the model for the system that performance surplus can be shared with any units with performance deficiency [7]. In recent years, MSS-CBPS has attracted increasing attention, with researchers extending models to analyze reliability and availability of different types of MSS-CBPS. The model has evolved from a series structure to K-out-of-n structure [8,9], linear sliding window structure [10]. The model with one common bus was also extended to the model with hierarchical or two performance sharing groups [11–14]. Moreover, the reliability model of phase mission system with common bus performance sharing, transmission loss of common bus, performance storage, and uncertainty were also studied [15–18]. Meanwhile, unpredictable and inevitable disturbances

* Corresponding author.
E-mail address: jiaojian@buaa.edu.cn (J. Jiao).

https://doi.org/10.1016/j.ress.2025.111040
Received 29 June 2024; Received in revised form 31 December 2024; Accepted 15 March 2025
Available online 16 March 2025

are common and can significantly impact system performance. The issue of the model under random shocks was also studied [19]. Following these existing studies, the Markov process is widely used to model the state transition process of components (e.g. [16,19]) and Universal Generating Function (UGF) is also an effective tool for analyzing the reliability and availability of multi-state system (e.g. [14]). Notably, due to the varying structures and operating mechanisms of different models, each model needs to develop its own UGF algorithm to analyze its reliability or availability.

In addition, with the widespread application of the system in the industry, it is essential to ensure the continuous and stable operation of these systems. Therefore, many researchers pay attention to the research of recovery strategies to enhance the system's ability to deal with random disturbances. Recent studies mostly focus on backup recovery strategies [20,21], defense strategies [22] and maintenance strategies [23]. However, for MSS-CBPS, performance reallocation mechanisms via the common bus are more effective in addressing random disturbances. Despite this, dynamic reconfiguration (a form of performance reallocation) has received limited attention in MSS-CBPS research due to its complexity. Therefore, incorporating dynamic reconfiguration into the modeling process for MSS-CBPS is crucial. Not only will this approach help fill existing research gaps, but it will also significantly enhance the system's ability to manage random disturbances.

Due to the research on recovery strategies and the model under random shocks, compared with reliability and availability, resilience may be more suitable to describe the system's capacity to resist, respond to, and recover from random disturbances, as it captures not only the system's ability to maintain functionality under disturbances but also its capacity to recover normal operation state after disturbances [24,25]. Therefore, it is essential to analyze the system from the resilience perspective, taking dynamic reconfiguration into account to enhance its ability to cope with the disturbances. For the multi-state system, the Markov process is commonly used to characterize mathematical models for resilience analysis. However, current research on resilience modeling based on the Markov process mainly focuses on independence between system components or evaluates the resilience of the multi-state system from a macro-level perspective [26–28].

In addition, previous researchers have also explored the issue of resilience assessment from various perspectives, including resilience assessment based on hazard and recovery time [29,30], resilience assessment based on performance variations within a time cycle [31], resilience assessment based on instantaneous performance [32–34], resilience assessment based on probabilistic indicators [35] and resilience assessment based on multiple indicators [36]. Despite these efforts, most quantification methods of multi-state systems primarily focus on using time metrics to analyze system resilience. These methods include either evaluating the probability that the system remains in a state for a duration exceeding the threshold [26,27] or calculating the ratio of the time the system spends in a given state to total operation time [28]. In conclusion, existing methods have not sufficiently addressed the critical feature of performance sharing among components in complex systems. The interdependence and multi-state characteristics of components can significantly impact the accuracy of system resilience assessment. Moreover, resilience assessment methods based on performance metrics have also received limited attention in research on the multi-state system.

Current research has made significant progress in modeling multi-state system with bus performance sharing, recovery strategies, and resilience assessment. However, several issues still require further investigation. First, while existing studies on MSS-CBPS primarily focus on reliability and availability modeling, resilience is better suited for describing the dynamic behavior of systems under random disturbances; this includes the system's ability to resist, respond to, and recover from disturbances. Second, there is limited research on resilience modeling and assessment in multi-state systems, particularly in terms of component interactions that arise from performance sharing mechanisms. These interactions can significantly impact the overall system performance. Meanwhile, the research on multi-state system resilience assessment based on performance metrics has received insufficient attention. Finally, although scholars have discussed maintenance strategies and redundancy recovery strategies in recovery strategies for MSS-CBPS, dynamic reconfiguration mechanisms have yet to be fully explored. These mechanisms enable systems to reallocate resources and restore normal operations when facing disturbances effectively.

Therefore, the paper focuses on two main aspects. On the one hand, based on the working principles of MSS-CBPS and dynamic reconfiguration, this paper introduces a novel model suitable for describing MSS-CBPS under dynamic reconfiguration. Additionally, it proposes a resilience model from the perspectives of resistance, response, and recovery resilience. On the other hand, based on the mentioned resilience model, a UGF-based resilience assessment algorithm is proposed to evaluate system resilience under dynamic reconfiguration. At the same time, this paper also studies the trends in system resilience under the component backup and recovery strategy and the resource preemption strategy to provide theoretical support for system resilience design.

The structure of this paper is organized as follows: The second section introduces a novel MSS-CBPS model that incorporates component importance and dynamic reconfiguration, along with an associated resilience assessment framework. The third part provides a UGF-based resilience assessment algorithm suitable for the system under the component backup and recovery strategy and the resource preemption strategy to evaluate the system resilience under different dynamic reconfiguration strategies. In the fourth part, the paper uses an integrated mission processing system in the integrated modular avionics (IMA) system of a helicopter as an example to verify the feasibility of the resilience modeling and evaluation method. The fifth part summarizes the entire paper and proposes potential future research directions.

2. Modeling descriptions

2.1. System structure model and mechanism

2.1.1. Multi-state system with common bus performance sharing

MSS-CBPS [6] consists of n multi-state units connected with a common bus, as illustrated in Fig. 1. Each unit in the system can operate in multiple states and has a random performance G_i to satisfy its random performance demand W_i. When there is performance surplus in the units, the surplus can be randomly shared with the units with performance deficiency through a common bus whose transmission capacity is C. To ensure the system works, each unit should have sufficient performance to satisfy its demand.

However, recent research has not considered the sequence of performance reallocation and dynamic reconfiguration. In system operation, when distributed performance is insufficient, the order in which performance is reallocated plays a crucial role in determining which disrupted units can recover to a functional state. If performance surplus is not allocated to critical units with system safety-affecting tasks, the system may become unsafe. Moreover, dynamic reconfiguration strategies have already been widely used in industry because they effectively enhance system resilience against random disturbances by reallocating resources. Therefore, it is critical to thoroughly explore the sequence of

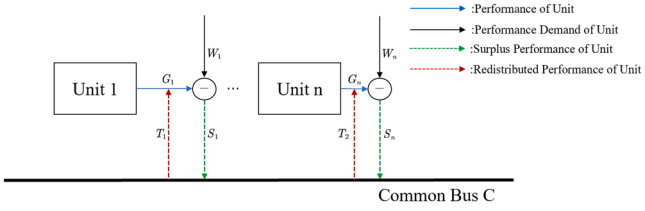

Fig. 1. Structure of MSS-CBPS.

performance allocation and dynamic reconfiguration during research on the MSS-CBPS problem.

2.1.2. Importance-based MSS-CBPS

The sequence of performance allocation directly affects whether the system can remain in a working, safe, or dangerous state in the face of unpredictable disturbances. To determine the sequence, the importance of the tasks in each unit needs to be considered to ensure that critical units can receive the necessary support in emergencies. Therefore, in the new structural model shown in Fig. 2, the units are divided into$n_1$major units and$n - n_1$minor units according to the performance of the units. Tasks are then assigned to the units in order of their importance, from the most critical to the least critical. When some units suffer from performance deficiency, units with performance surplus can allocate distributed performance via a common bus to these units, prioritizing based on the importance of the tasks each unit performs, from most critical to least critical, to manage internal and external disturbances. The transmission capacity of the common bus is limited, and the maximum is$C$.

2.1.3. System mechanism

Dynamic reconfiguration, as a common resilience recovery strategy, can effectively enhance the system's ability to handle disturbances. It is also an essential factor and cannot be overlooked. Therefore, based on the importance-based MSS-CBPS structure model, two dynamic reconfiguration strategies, component backup and recovery, and resource preemption are incorporated to further develop the structural model.

(1) Component backup and recovery strategy

The component backup and recovery strategy is illustrated in Fig. 3. When units in the system experience performance deficiency and a sufficient number of backup units are available, the units with performance deficiency can request assistance from the backup units, with resource allocation prioritized based on task importance, from highest to lowest. For example, suppose the performance of Major Unit 1 and Minor Unit n cannot meet the performance demand of their tasks. In the case, the system prioritizes allocating the resource of the backup unit to Major Unit 1. Once the demand for Major Unit 1 is satisfied and if there is remaining transmission capacity on the bus and available backup units, Minor Unit n is allowed to utilize the resources of the backup units. The system is restored to normal when the performance of the backup units meets the demands of the disturbed units and the number of operational units matches the specified system requirements.

(2) Resource Preemption strategy

The resource preemption strategy is illustrated in Fig. 4. When no backup units are available in the system to meet the demand of units with performance deficiency, the system terminates the task assigned to the nth unit and reallocates its performance to other units with performance deficiency. For example, if Major Unit 1 cannot meet the performance demand due to a failure, the system terminates the task assigned to Minor Unit n and reallocates its resource to satisfy the performance demand of Major Unit 1. Once the performance demands of other deficient units except for nth unit are met, the system restores to a safe state. Moreover, the transmission capacity of resources during the resource preemption strategy process is also limited.

2.2. System mathematical description

The Markov process is widely applied in resilience analysis to model the state transition process (e.g. [27,28]). In this paper, we examine a multi-state system that is non-repairable, where failures result in transitions of the units or the bus from high-performance states to low-performance states. Since the future states of the units and the bus depend only on their current states, the performance of the units and the transmission capacity of the bus can be represented by a continuous-time discrete-state Markov process (Fig. 5).

Next, the Kolmogorov function is used to obtain the probabilities of the performance of the units and the transmission capacity of the bus in different states.

$$\frac{d\alpha_i(t)}{dt} = \alpha_i(t) * Q_i \tag{1}$$

where,$\alpha_i(t)$represents the probabilities of units or the bus in every state, and$Q_i$is state transition probability density matrix, which can be described as

$$Q_i = \begin{Bmatrix} \lambda_{H_i,H_i} & \lambda_{H_i,H_i-1} & \cdots & \lambda_{H_i,1} \\ 0 & \lambda_{H_i-1,H_i-1} & \cdots & \lambda_{H_i-1,1} \\ \vdots & \vdots & \ddots & \vdots \\ 0 & 0 & \cdots & \lambda_{1,1} \end{Bmatrix} \tag{2}$$

Furthermore, random disturbances increase the rate of state transitions rates, particularly accelerating degradation from higher performance state to lower performance states.

When the total performance of units exceeds their demand, the performance surplus can be redistributed to units with performance deficiency through the common bus. Therefore, based on the performance and demand of the units in the system, the mathematical expressions for the performance surplus and deficiency at any given time are as follows:

$$S_i(t) = \max(G_i(t) - W_i(t), 0) \tag{3}$$

$$D_i(t) = \max(W_i(t) - G_i(t), 0) \tag{4}$$

The vector of performance surplus$S$and performance deficiency$D$for the system can be described as

$$S = [S_1(t), S_2(t), \ldots, S_n(t)] \tag{5}$$

$$D = [D_1(t), D_2(t), \ldots, D_n(t)] \tag{6}$$

When the performance surplus is redistributed to the units with

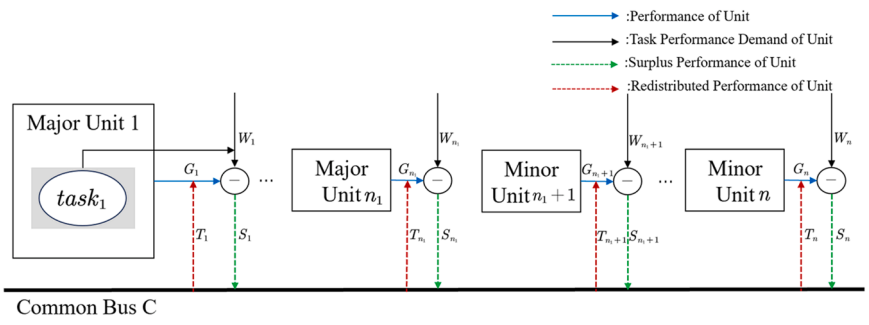

Fig. 2. Importance-based MSS-CBPS structure.

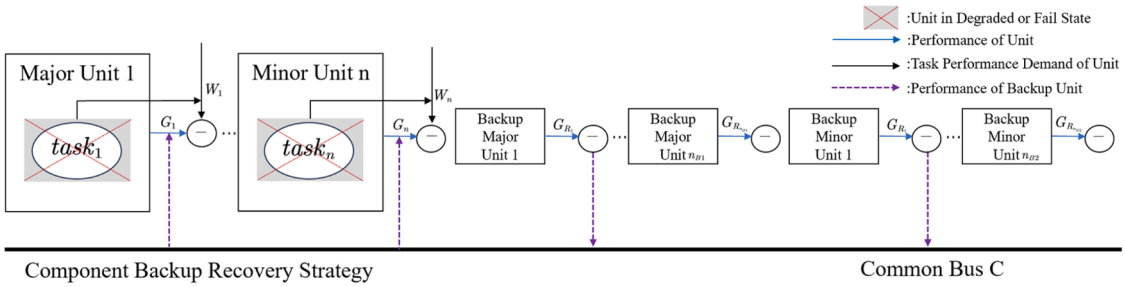

Fig. 3. Schematic diagram of the component backup and recovery strategy.

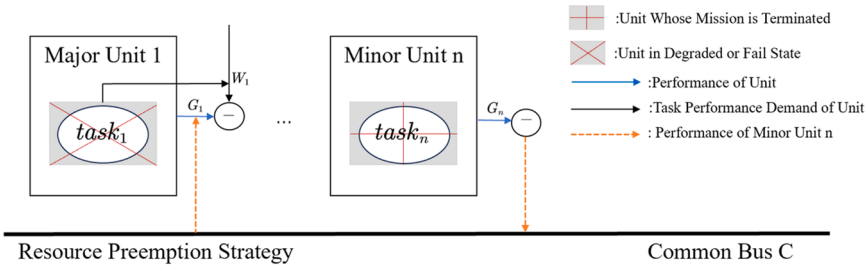

Fig. 4. Schematic diagram of the resource preemption strategy.

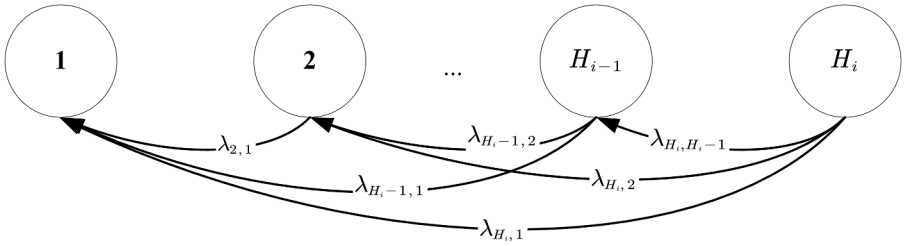

Fig. 5. Markov model.

performance deficiency through the common bus, the transmitted performance is.

$$T(t) = \min\left(\sum_{i=1}^{n} S_i(t), C(t)\right) = \min\left(\sum_{i=1}^{n} \max(G_i(t) - W_i(t), 0), C(t)\right) \tag{7}$$

To maintain the operational functionality of units assigned to more critical tasks, the redistributable performance is allocated in a prioritized sequence that reflects the importance of the tasks assigned to each unit. The vector$\widetilde{D}$representing performance deficiency under performance sharing can be derived using the algorithm presented in Table 1.

$$\widetilde{D} = [\widetilde{D}_1(t), \widetilde{D}_2(t), ..., \widetilde{D}_n(t)] \tag{8}$$

Upon activating the performance sharing mechanism in response to disturbances, the system initiates either the component backup and recovery strategy or the resource preemption strategy to facilitate recovery. To evaluate the recovery effectiveness of each strategy, mathematical formulations are developed to quantify the remaining performance deficiency.

(1) System performance deficiency model under the component backup and recovery strategy

According to Algorithm 2, presented as Table 2, the performance deficiency vector$\overline{D}$for each unit under the component backup and recovery strategy can be derived.

Table 1
Algorithm for performance sharing.

Algorithm 1: Flow of performance sharing
1: Input: Redistributed performance $T(t)$and performance deficiency vector D
2: Output: Performance deficiency vector under performance sharing $\widetilde{D}$
3: **for** every element in performance deficiency vector from $D_1(t)$to$D_n(t)$
$\widetilde{D}_i(t)$=max$(D_i(t) - T(t), 0)$
$T(t) = \max(T(t) - D_i(t), 0)$
if $i > n$
end for
4: Put $\widetilde{D}_1(t), \widetilde{D}_2(t), ..., \widetilde{D}_n(t)$into $\widetilde{D}$
5: Return Performance deficiency vector under performance sharing $\widetilde{D}$

Table 2
Algorithm for performance sharing under the component backup and recovery strategy.

Algorithm 2: Flow of performance sharing under the component backup and recovery strategy
1: Input: Transportation capacity $C(t)$, Performance deficiency vector D,Performance surplus vector S, and Performance vector of backup component S_R
2: Output: Performance deficiency vector under the component backup and recovery strategy $\overline{D}$
3: Distributed performance surplus $T(t) = \min\left(\sum S + \sum S_R, C(t)\right)$
for every element in performance deficiency vector from $D_1(t)$ to $D_n(t)$
$\overline{D}_i(t)$=max$(D_i(t) - T(t), 0)$
$T(t) = \max\left(T(t) - D_i(t), 0\right)$
if $i > n$
end for
4: Put $\overline{D}_1(t), \overline{D}_2(t), \ldots, \overline{D}_n(t)$ into $\overline{D}$
5: Return Performance deficiency vector $\overline{D}$

$$\overline{D} = [\overline{D}_1(t), \overline{D}_2(t), \ldots, \overline{D}_n(t)] \tag{9}$$

(2) System performance deficiency model under the resource preemption strategy

According to Algorithm 3, presented as Table 3, the performance deficiency vector$\widehat{D}$for each unit under the resource preemption strategy can be derived.

$$\widehat{D} = [\widehat{D}_1(t), \widehat{D}_2(t), \ldots, \widehat{D}_{n-1}(t)] \tag{10}$$

2.3. System resilience model

Resilience modeling is a core component in the study of industry system resilience and is continuous to be studied [37]. Resilience has been regarded as the integration of several resilience factors, including resistance, absorption, and recovery [27,28]; the interaction of cumulative loss and gain of functionality [38]; the combination of resistance, adaptability, and recovery [39]; and the integration of reliability, redundancy, robustness, and recovery [40]. For the operation mechanism of MSS-CBPS, when it is disrupted, it will actively response to the random disturbances. Based on these existing works and the operation mechanism of MSS-CBPS, resilience can be understood as the ability of a system to resist respond to disturbances and recover quickly after being impacted. Moreover, a unified resilience assessment framework is essential, as resilience needs to be evaluated through multiple indicators. Therefore, we comprehensively measure the system resilience under dynamic reconfiguration from three aspects: resistance resilience, response resilience, and recovery resilience, shown in Fig. 6 [5].

(1) Resistance resilience$\Re_d$

Resistance resilience$\Re_d$mainly represents the ability of the system to prevent or withstand random disturbances, and it can be measured by the system reliability. Specifically, it can be described as the success rate of the system resisting disturbances.

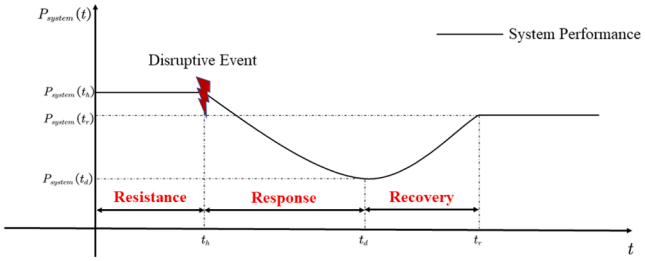

Fig. 6. Performance tendency of the system.

$$\begin{aligned}\Re_d &= \frac{N - N_f}{N} \\ &= \Pr\left\{\sum_{i=1}^{n} D_i(t) = 0, N_1 \geq \overline{n}_1, N_2 \geq \overline{n}_2\right\}\end{aligned} \tag{11}$$

where,$N$is the frequency of disturbances, and$N_f$is the frequency at which the system fails to resist disturbances.$N_1$and$N_2$is the number of major units and the number of minor units in a working state, respectively.$\overline{n}_1$and$\overline{n}_2$is the specified number of major units and the specified number of minor units when the system is in a working state, respectively .

(2) Response resilience$\Re_x$

Response resilience$\Re_x$mainly represents the ability of the system to actively respond to the disturbances through performance sharing after the failure of system resistance. This capability enables the system to maintain essential functions and remain operational temporarily, which demonstrates characteristics similar to robustness [5,39,41]. Response resilience can be considered the incremental probability of the system being in a working state under the bus performance sharing.

Table 3
Algorithm for performance sharing under the resource preemption strategy.

Algorithm 3: Flow of performance sharing under the resource preemption strategy
1: Input: Transportation capacity $C(t)$, Performance deficiency vector D, Performance surplus vector S, and Performance of component n, $G_n(t)$
2: Output: Performance deficiency vector under the resource preemption strategy $\widehat{D}$
3: Distributed performance surplus $T(t) = \min\left(\sum_{i=1}^{n-1} S_i(t) + G_n(t), C(t)\right)$
for every element in performance deficiency vector from $D_1(t)$ to $D_n(t)$
$\widehat{D}_i(t)$=max$(D_i(t) - T(t), 0)$
$T(t) = \max\left(T(t) - D_i(t), 0\right)$
if $i > n - 1$
end for
4: Put $\widehat{D}_1(t), \widehat{D}_2(t), \ldots, \widehat{D}_{n-1}(t)$ into $\widehat{D}$
5: Return Performance deficiency vector $\widehat{D}$

$$\Re_x = P_{share} - P_{sys} = \Pr\left\{\sum_{i=1}^{n} \widetilde{D}_i(t) = 0\right\} - \Pr\left\{\sum_{i=1}^{n} D_i(t) = 0, N_1 \geq \overline{n}_1, N_2 \geq \overline{n}_2\right\} \quad (12)$$

where,$P_{share}$is the probability of the system remaining operational under common bus performance sharing, and$P_{sys}$is the probability of the system being in a working state without considering common bus performance sharing.

(3) Recovery resilience$\Re_h$

Recovery resilience$\Re_h$ primarily reflects the ability of the system to recover performance through dynamic reconfiguration strategies after responding to the disturbances. It is characterized by the incremental probability of the system transitioning in a working or safe state.

$$\Re_h = P_{dyn} - P_{sys} \quad (13)$$

where,$P_{dyn}$is the probability of the system being in a working or safe state under dynamic reconfiguration strategies.

The recovery resilience$\Re_{h_1}$under the component backup and recovery strategy is

$$\Re_{h_1} = \Pr\left\{\sum_{i=1}^{n} \overline{D}_i(t) = 0, \overline{N}_1 \geq \overline{n}_1, \overline{N}_2 \geq \overline{n}_2\right\} - \Pr\left\{\sum_{i=1}^{n} D_i(t) = 0, N_1 \geq \overline{n}_1, N_2 \geq \overline{n}_2\right\} \quad (14)$$

where,$\overline{N}_1$and$\overline{N}_2$are the number of major units and the number of minor units in a working state under the component backup and recovery strategy, respectively.

The recovery resilience$\Re_{h_2}$under the resource preemption strategy is

$$\Re_{h_2} = \Pr\left\{\sum_{i=1}^{\hat{n}} \widehat{D}_i(t) = 0\right\} - \Pr\left\{\sum_{i=1}^{n} D_i(t) = 0, N_1 \geq \overline{n}_1, N_2 \geq \overline{n}_2\right\} \quad (15)$$

In this paper, resilience quantification involves a unified framework for comprehensively evaluating system resistance, response, and recovery resilience while considering these factors as independent components [42]. This paper measures system resilience through the probabilistic quantification of resistance resilience, response resilience, and recovery resilience, as detailed below:

$$\Re_{system} = \Re_d + \Re_x \times (1 - \Re_d) + \Re_h \times (1 - \Re_d) \times (1 - \Re_x) \quad (16)$$

3. System resilience calculation

3.1. System resistance resilience calculation

The Universal Generating Function (UGF) method proposed by Ushakov offers notable advantages over other methods such as Monte Carlo simulation models for calculating state probabilities in MSS-CBPS. By utilizing a concise and intuitive recursive process, the UGF method efficiently represents system performance levels and calculates the performance distribution probabilities of multi-state systems [43]. This method has been widely applied in MSS-CBPS analyses (e.g. [14,19]) and is demonstrates particular efficiency in resilience assessments of complex multi-state systems. Therefore, given its suitability for analyzing MSS-CBPS, we use the UGF method to quantitatively evaluate the resilience of MSS-CBPS under various dynamic reconfiguration strategies.

Additionally, as the operational state of the system depends on both the operational state of its units and the satisfaction of performance demand, this paper employs a bivariate universal generating function [9] to represent the probability mass function (pmf) of unit performance and demand in UGF form.

Performance$G_i$of unit$i$is randomly obtained from vector$\left[g_{i,1}, g_{i,2}, \ldots, g_{i,h_i}\right]$, and the pmf of performance$G_i$in UGF form is.

$$u_i(z_1, z_2) = \sum_{h=1}^{h_i} \alpha_{i,h} z_1^{g_{i,h}} z_2^{u_{i,h}} \quad (17)$$

where,$\alpha_{i,h}$is the probability that the performance of unit$i$is$g_{i,h}$,and the operation state is$u_{i,h}$.When$g_{i,h} > 0$,$u_{i,h} = 1$; when$g_{i,h} \leq 0$,$u_{i,h} = 0$.

Demand$W_i$of unit$i$ is randomly obtained from vector $\left[w_{i,1}, w_{i,2}, \ldots, w_{i,p_i}\right]$, and the pmf of demand$W_i$in UGF form is

$$\omega_i(z_1, z_2) = \sum_{p=1}^{p_i} \beta_{i,p} z_1^{w_{i,p}} z_2^{\omega_{i,p}} \quad (18)$$

where, $\beta_{i,p}$is the probability that the demand of unit$i$is$w_{i,p}$, and the requirement of the operation state is$\omega_{i,p}$.When$w_{i,p} \geq 0$,$\omega_{i,p} = 1$.

Eq. (3) is used to calculate the performance surplus of unit$i$, and Eq. (4) is used to calculate the performance deficiency of unit$i$. Next, the combination operator$\otimes$ is used to obtain the joint UGF of the performance surplusS_i,performance deficiencyD_i,and operation stateF_i.

$$\begin{aligned}\Delta_i(z_1, z_2) &= u_i(z_1, z_2) \otimes \omega_i(z_1, z_2) \\ &= \sum_{v=1}^{V_i} \zeta_{i,v} z_1^{\max\left(g_{i,h} - w_{i,p}, 0\right), \max\left(w_{i,p} - g_{i,h}, 0\right)} z_2^{u_{i,h} - \omega_{i,p}} \\ &= \sum_{v_i=1}^{V_i} \zeta_{i,v_i} z_1^{s_{i,v_i}, d_{i,v_i}} z_2^{F_{i,m,v_i}}\end{aligned} \quad (19)$$

where,$V_i$is the number of terms in the UGF after collecting like terms,s_{i,v_i} andd_{i,v_i}represent the performance surplus and performance deficiency of unit$i$,respectively.$F_{i,m,v_i}$is the operation state of unit$i$, and subscript$m$is used to distinguish between the unit is a major unit ($m = 1$) and minor unit ($m = 2$). If$u_{i,h} - \omega_{i,p} = 0$, unit$i$is in a working state, andF_{i,m,v_i}can be written as$F_{i,m,v_i}^{[1]}$. Otherwise, it is in a failure state,$F_{i,m,v_i}$is written as$F_{i,m,v_i}^{[0]}$,and$\zeta_{i,v_i}$is the joint event probability, which can be written as$\zeta_{i,v} = \Pr\left\{S_i = s_{i,v_i}, D_i = d_{i,v_i}, F_i = F_{i,m,v_i}\right\}$.

For the whole system, the operator$\underset{+}{\oplus}$is used for iterative calculations to obtain the UGF of the vector of performance surplus$S$, performance deficiency$D$and operation state$F$.

$$\begin{aligned}U_\Omega(z_1, z_2) &= \Delta_1(z_1, z_2) \underset{+}{\oplus} \Delta_2(z_1, z_2) \underset{+}{\oplus} \ldots \underset{+}{\oplus} \Delta_i(z_1, z_2) \\ &= \sum_{v_1=1}^{V_1} \sum_{v_2=1}^{V_2} \ldots \sum_{v_n=1}^{V_n} \left(\prod_{i=1}^{n} \zeta_{i,v_i}\right) z_1^{\bigcup s_{i,v_i}, \bigcup d_{i,v_i}} z_2^{\bigcup (F_{i,m,v_i})} \\ &= \sum_{j=1}^{A_j} \pi_{A,j} z_1^{s_{A,j}, d_{A,j}} z_2^{F_{A,j}}\end{aligned} \quad (20)$$

where$A_j$is the number of terms in the UGF after collecting like terms,$s_{A,j}$ and$d_{A,j}$are the performance surplus vector and the performance deficiency vector for each unit in the system, respectively. $F_{A,j} = \left[F_{1,1,j}, F_{2,1,j}, \ldots, F_{n_1,1,j}, F_{n_1+1,2,j}, F_{n_2+2,2,j}, \ldots, F_{n,2,j}\right]$is the operation state vector for each unit in the system. The joint event probability$\pi_{A,j}$can be described as$\Pr\left\{S = s_{A,j}, D = d_{A,j}, F = F_{A,j}\right\}$.

According to Eqs. (11) and (20), the resistance resilience$\Re_d$can be written as

$$\Re_d = \Pr\left\{\sum d_{A,j} = 0, \sum_{i=1}^{n_1} I\left(F_{i,1,j} = F_{i,1,j}^{[1]}\right) \geq \overline{n}_1, \sum_{i=n_1+1}^{n} I\left(F_{i,2,j} = F_{i,2,j}^{[1]}\right) \geq \overline{n}_2\right\} \quad (21)$$

where,$I()$is the indicative function.

3.2. System responsiveness resilience calculation

The system responds to internal or external disturbances through the performance sharing mechanism. The transmission capacity$C$is obtained from vector$[c_1, c_2, \ldots c_K]$. The UGF of transmission capacity$C$is

$$\eta(z_1) = \sum_{k=1}^{K} \delta_k z^{c_k} \tag{22}$$

where,$\delta_k = Pr\{c = c_k\}$.

According to Eqs. (20) and (22), using the algorithm of performance sharing (Table 1), the UGF of the performance deficiency vector$\widetilde{D}$is

$$\begin{aligned}\widetilde{U}_A(z_1, z_2) &= U_\Omega(z_1, z_2) \odot \eta(z_1) \\ &= \sum_{j=1}^{A_j} \sum_{k=1}^{K} \pi_{A,j} \delta_k z_1^{\tilde{d}_{A,j}} z_2^{F_{A,j}} \\ &= \sum_{j_a=1}^{J_A} P_{j_a} z_1^{\tilde{d}_{j_a}} z_2^{F_{j_a}}\end{aligned} \tag{23}$$

where,$J_A$is the number of terms in the UGF after collecting like terms, and$P_{j_a}$is the joint probability, which can be represented as $P_{j_a} = \Pr\{\widetilde{D} = \widetilde{d}_{j_a}, F = F_{j_a}\}$.

According to Eqs. (12), (21) and (23), the response resilience$\Re_x$is

$$\Re_x = \Pr\left\{\sum \widetilde{d}_{j_a} = 0\right\} - \Re_d \tag{24}$$

3.3. System recovery resilience calculation

3.3.1. System recovery resilience calculation under the component backup and recovery strategy

After the system responds to internal and external disturbances through the performance sharing mechanism, it recovers to a working state or a safe state by triggering the component backup and recovery strategy or the resource preemption strategy. According to the component backup and recovery strategy, using the combination operator$\odot$, the UGF form of the performance deficiency vector$\overline{D}$can be calculated as

$$\overline{U}_B(z_1, z_2) = U_{\Omega_1}(z_1, z_2) \odot \eta(z_1) \tag{25}$$

$$= \sum_{j_b=1}^{J_B} p_{j_b} z_1^{\overline{d}_{j_b}} z_2^{F_{j_b}}$$

where, $U_{\Omega_1}(z_1, z_2)$is the UGF form of the joint pmf for the vector of performance surplus, deficiency, and operation state under the component backup and recovery strategy.$J_B$is the number of terms in the UGF after collecting like terms. $\overline{d}_{j_b}$is the vector of the unit with performance deficiency under the component backup and recovery strategy, and$P_{j_b}$is the joint event probability, which can be represented as $P_{j_b} = \Pr\{\overline{D} = \overline{d}_{j_b}, F = F_{j_b}\}$.

F_{j_b}consists of$F_{j_{b1}}$and$F_{j_{b2}}$,$F_{j_{b1}}$is the operation state vector of major units and their corresponding invoked backup units, $F_{j_{b2}}$is the operation state vector of minor units and their corresponding invoked backup units.

$$F_{j_{b1}} = \left[F_{1,1}, F_{2,1}, \ldots, F_{L_1,1}\right] \tag{26}$$

$$F_{j_{b2}} = \left[F_{1,2}, F_{2,2}, \ldots, F_{L_2,2}\right] \tag{27}$$

According to Eqs. (14) and (25), the recovery resilience$\Re_{h_1}$of the system under the component backup and recovery strategy is

$$\Re_{h_1} = Pr\left\{\sum \overline{d}_{j_b} = 0, \sum_{l=1}^{L_1} I\left(F_{l,1} = F_{l,1}^{[1]}\right) \geq \overline{n}_1, \sum_{l=1}^{L_2} I\left(F_{l,2} = F_{l,2}^{[1]}\right) \geq \overline{n}_2\right\} - \Re_d \tag{28}$$

3.3.2. System recovery resilience under the resource preemption strategy

Similarly, the UGF for the performance deficiency vector$\widehat{D}$ under the resource preemption strategy can be represented as.

$$\widehat{U}_E(z_1, z_2) = \sum_{j_e=1}^{J_E} p_{j_E} z_1^{\hat{d}_{j_e}} z_2^{F_{j_e}} \tag{29}$$

where, $\widehat{d}_{j_e}$is the vector of the performance deficiency of the units undertaking tasks affecting system safety, and$F_{j_e}$is the operation state vector of the units.

According to Eqs. (15) and (29), the recovery resilience of the system under the resource preemption strategy is.

$$\Re_{h_2} = Pr\left\{\sum \widehat{d}_{j_e} = 0\right\} - \Re_d \tag{30}$$

3.4. The algorithm for system resilience assessment

System resilience under dynamic reconfiguration$\Re_{system}$is obtained according to Eq. (16) after resistance resilience$\Re_d$,responsiveness resilience$\Re_x$, and recovery resilience$\Re_h$are calculated. The procedures for the system resilience assessment based UGF is tabulated in Table 4.

4. Case study

The integrated task processing system is a core system of the integrated modular avionics in helicopters. It is primarily responsible for processing data from components such as night vision and surveillance equipment and providing pilots with the necessary parameters. The system comprises several general processing units (GPUs), categorized into major and minor GPUs, connected via a communication bus. Major GPUs handle more critical tasks directly related to system safety, while minor GPUs take care of the rest. Each GPU is responsible for handling tasks, with its task processing capacity representing its performance and the tasks it manages reflecting its demand. During the mission, if one GPU is degraded or disturbed, the GPUs with high task processing speed or low task demand can help the degraded or disturbed GPU with insufficient task processing ability through the communication system to ensure continued functionality. Due to the critical role of the task processing system in maintaining helicopter functionality and safety, improving its resilience is important. Dynamic reconfiguration mechanisms, such as component backup and recovery strategy and resource preemption strategy, effectively address thses challenges. The component backup and recovery strategy involves replacing the GPUs that insufficient task processing ability with spare GPUs. Moreover, the resource preemption strategy is when neither major GPUs nor spare GPUs can work; the resources for minor tasks are allocated to major tasks to maintain system safety.

Moreover, based on the operation mechanism of the system, the task processing system can be viewed as a multi-state system with common bus performance sharing (MSS-CBPS) under dynamic reconfiguration mechanisms. The resilience model and assessment method proposed in the paper are well-suited for analyzing the system's resilience under different dynamic reconfiguration strategies, highlighting the critical role the strategies play in enhancing system resilience.

The detail of the task processing system is set as follows. The system consists of one major general processing unit I (GPU I), one minor general processing unit II (GPU II), and a backup general processing unit I, as shown in Fig. 7. When one GPU is disturbed, the system quickly

Table 4
The algorithm for system resilience assessment based on the UGF.

Algorithm 4: System resilience assessment based on UGF
1: Input: The pmf of G_i,$W_i$and C, the number of components n.
2: Output: System resilience $\Re_{system}$ under dynamic reconfiguration.
3: **for** $i = 1, 2, \ldots, n$ do Calculate the UGF of G_i by using Eq. (17) Calculate the UGF of W_i by using Eq. (18) **end for**
4: **for** $i = 1, 2, \ldots, n$ do Calculate the UGF of performance surplus S_i and performance deficiency D_i for component$i$, $\Delta_i(z_1, z_2)$based on Eq. (19) Calculate the UGF of performance surplus vector $S$and performance deficiency vector D for system, $U_\Omega(z_1, z_2)$by using Eq. (20) **end for**
5: Calculate resistance resilience $\Re_d$by using Eq. (21), based on Eq. (11) and the result of Eq. (20)
6: Calculate the UGF of C by using Eq. (22)
7: Calculate the UGF of performance deficiency vector $\widetilde{D}$ for the system under common bus performance sharing by using Eq. (23) based on **Algorithm 1**
8: Calculate responsiveness resilience $\Re_x$ by using Eq. (24), based on Eq. (12) and the result of Eq. (23)
9: Calculate the UGF of performance deficiency vector $\overline{D}$ for the system under component backup and recovery strategy by using Eq. (25) based on **Algorithm 2**
10: Calculate recovery resilience $\Re_{h_1}$ by using Eq. (28), based on Eq. (14) and the result of Eq. (25)
11: Calculate the UGF of performance deficiency vector $\widehat{D}$ for the system under resource preemption strategy by using Eq. (29) based on **Algorithm 3**
12: Calculate recovery resilience $\Re_{h_2}$ by using Eq (30), based on Eq. (15) and the result of Eq. (29)
13: Calculate system resilience under component backup and recovery strategy $\Re_{system_1}$ by combining$\Re_d$, $\Re_x$, and $\Re_{h_1}$ according to Eq. (16)
14: Calculate system resilience under resource preemption strategy$\Re_{system_2}$ by combining$\Re_d$, $\Re_x$, and $\Re_{h_2}$ according to Eq. (16)
15: Return system resilience $\Re_{system_1}$ and $\Re_{system_2}$

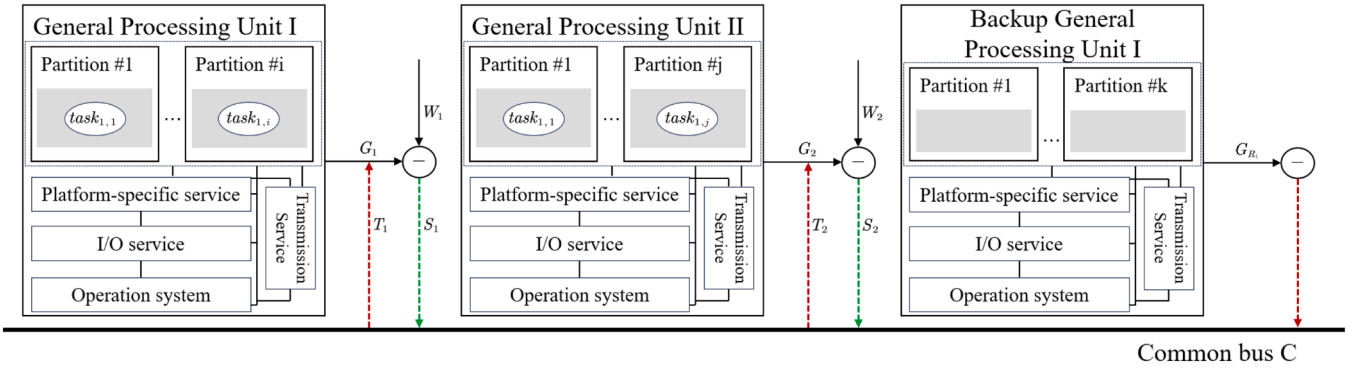

Fig. 7. The structure of the integrated task process system in the helicopter.

responds to random disturbances through performance sharing. Then, dynamic reconfiguration strategies are triggered to enable the system to recover to a working or safe state.

When the system works, both GPU I and GPU II need to work. When the system fails but is in a safe state, GPU II can terminate its tasks due to the failure or the resource preemption strategy. When one GPU breaks down, the time of responding to a failure and the time of recovering from a failure by triggering dynamic reconfiguration are 10 s. And according to the ASAAC standard, the IMA does not require maintenance in at least 150 h [44]. Therefore, the influence of maintenance on system resilience is not considered. The details of the GPUs and the common bus are tabulated as Tables 5-7.

(1) The UGF form of performance and demand of each GPU in the system is

Table 6
The demand, state probability and importance of the GPU.

GPU i			Probability	Initial condition	Importance
i	Demand	Demand level			
1	1	L2	0.1	0	I
	2	L1	0.9	1	I
2	0	L2	0.1	0	II
	1	L1	0.9	1	II

Table 5
Performance, transition intensities and importance of the GPU.

GPU i			Transition intensities			Initial condition	Importance
i	Performance	Performance level	L1	L2	L3		
1	0	L1	0	0	0	0	I
	2	L2	0.0001	−0.0001	0	0	I
	4	L3	0.0005	0.0003	−0.0008	1	I
2	0	L1	0	0	–	0	II
	2	L2	0.0005	−0.0005	–	1	II

Table 7
Transmission capacity and transition intensities of the common bus.

Common bus			Transition intensities			Initial condition
	Transmission capacity C_i	Performance level	C1	C2	C3	
Common bus	0	C1	0	0	0	0
	1	C2	0.0001	−0.0001	0	0
	4	C3	0.0005	0.0003	−0.0008	1

GPU I: $u_1(z_1,z_2) = P_{G_{1,3}} z_1^{\,4} z_2^{\,1} + P_{G_{1,2}} z_1^{\,2} z_2^{\,1} + P_{G_{1,1}} z_1^{\,0} z_2^{\,0}$

$\omega_1(z_1,z_2) = P_{W_1} z_1^{\,2} z_2^{\,-1} + P_{W_2} z_1^{\,1} z_2^{\,-1}$

where, $P_{G_{1,3}} = e^{-0.0008t}$, $P_{G_{1,2}} = \frac{3}{7}\left[e^{-0.0001t} - e^{-0.0008t}\right]$, $P_{G_{1,1}} = 1 - P_{G_{1,3}} - P_{G_{1,2}}$, $P_{W_1} = 0.9$, and $P_{W_2} = 0.1$.

GPU II: $u_2(z_1,z_2) = P_{G_{2,2}} z_1^{\,2} z_2^{\,1} + P_{G_{2,1}} z_1^{\,0} z_2^{\,0}$

$\omega_2(z_1,z_2) = P_{W_1} z_1^{\,1} z_2^{\,-1} + P_{W_2} z_1^{\,0} z_2^{\,-1}$

where, $P_{G_{2,2}} = e^{-0.0005t}$, and $P_{G_{2,1}} = 1 - e^{-0.0005t}$.

(2) The UGF of performance surplus S_i and deficiency D_i of each GPU is

GPU I: $\Delta_1(z_1,z_2) = u_1(z_1,z_2) \underset{\Leftrightarrow}{\otimes} \omega_1(z_1,z_2)$

$P_{G_{1,3}}P_{W_2} z_1^{[3,0]} z_2^{F_{1,1}[1]} + P_{G_{1,3}}P_{W_1} z_1^{[2,0]} z_2^{F_{1,1}[1]} + P_{G_{1,2}}P_{W_2} z_1^{[1,0]} z_2^{F_{1,1}[1]}$

$P_{G_{2,1}}P_{W_2} z_1^{[0,0]} z_2^{F_{2,2}[0]} + P_{G_{2,1}}P_{W_1} z_1^{[0,1]} z_2^{F_{2,2}[0]}$

Backup GPU I: $\Delta_{R_1}(z_1,z_2) = u_{R_1}(z_1,z_2) \underset{\Leftrightarrow}{\otimes} \omega_{R_1}(z_1,z_2) =$

$P_{G_{1,3}} z_1^{[4,0]} z_2^{F_{R,1}[1]} + P_{G_{1,2}} z_1^{[2,0]} z_2^{F_{R,1}[1]} + P_{G_{1,1}} z_1^{[0,0]} z_2^{F_{R,1}[0]}$

The UGF of the transmission ability of the common bus is

$\eta(z_1) = P_{C_1} z_1^{\,0} + P_{C_2} z_1^{\,1} + P_{C_3} z_1^{\,4}$

where, $P_{C_3} = e^{-0.0008t}$, $P_{C_2} = \frac{3}{7}\left[e^{-0.0001t} - e^{-0.0008t}\right]$, and $P_{C_1} = 1 - P_{C_2} - P_{C_3}$.

(3) The performance surplus vector S and performance deficiency vector D are obtained by iterative calculation using the operator $\underset{+}{\oplus}$

$$
\begin{aligned}
&U_\Omega(z_1,z_2) = \Delta_1(z_1,z_2) \underset{+}{\oplus} \Delta_2(z_1,z_2) \\
&= \left(P_{G_{1,3}}\right)\left(P_{G_{2,2}}\right)\left(P_{W_2}\right)^2 z_1^{[3,2],[0,0]} z_2^{F_{1,1}[1],F_{2,2}[1]} + \left(P_{G_{1,3}}\right)\left(P_{G_{2,2}}\right)\left(P_{W_1}\right)\left(P_{W_2}\right) z_1^{[3,1],[0,0]} z_2^{F_{1,1}[1],F_{2,2}[1]} + \\
&\left(P_{G_{1,3}}\right)\left(P_{G_{2,1}}\right)\left(P_{W_2}\right)^2 z_1^{[3,0],[0,0]} z_2^{F_{1,1}[1],F_{2,2}[0]} + \left(P_{G_{1,3}}\right)\left(P_{G_{2,1}}\right)\left(P_{W_1}\right)\left(P_{W_2}\right) z_1^{[3,0],[0,1]} z_2^{F_{1,1}[1],F_{2,2}[0]} + \\
&\left(P_{G_{1,3}}\right)\left(P_{G_{2,2}}\right)\left(P_{W_1}\right)\left(P_{W_2}\right) z_1^{[2,2],[0,0]} z_2^{F_{1,1}[1],F_{2,2}[1]} + \left(P_{G_{1,3}}\right)\left(P_{G_{2,2}}\right)\left(P_{W_1}\right)^2 z_1^{[2,1],[0,0]} z_2^{F_{1,1}[1],F_{2,2}[1]} + \\
&\left(P_{G_{1,3}}\right)\left(P_{G_{2,1}}\right)\left(P_{W_1}\right)\left(P_{W_2}\right) z_1^{[2,0],[0,0]} z_2^{F_{1,1}[1],F_{2,2}[0]} + \left(P_{G_{1,3}}\right)\left(P_{G_{2,1}}\right)\left(P_{W_1}\right)^2 z_1^{[2,0],[0,1]} z_2^{F_{1,1}[1],F_{2,2}[0]} + \\
&\left(P_{G_{1,2}}\right)\left(P_{G_{2,2}}\right)\left(P_{W_2}\right)^2 z_1^{[1,2],[0,0]} z_2^{F_{1,1}[1],F_{2,2}[1]} + \left(P_{G_{1,2}}\right)\left(P_{G_{2,2}}\right)\left(P_{W_1}\right)\left(P_{W_2}\right) z_1^{[1,1],[0,0]} z_2^{F_{1,1}[1],F_{2,2}[1]} + \\
&\left(P_{G_{1,2}}\right)\left(P_{G_{2,1}}\right)\left(P_{W_2}\right)^2 z_1^{[1,0],[0,0]} z_2^{F_{1,1}[1],F_{2,2}[0]} + \left(P_{G_{1,2}}\right)\left(P_{G_{2,1}}\right)\left(P_{W_1}\right)\left(P_{W_2}\right) z_1^{[1,0],[0,1]} z_2^{F_{1,1}[1],F_{2,2}[0]} + \\
&\left(P_{G_{1,2}}\right)\left(P_{G_{2,2}}\right)\left(P_{W_1}\right)\left(P_{W_2}\right) z_1^{[0,2],[0,0]} z_2^{F_{1,1}[1],F_{2,2}[1]} + \left(P_{G_{1,2}}\right)\left(P_{G_{2,2}}\right)\left(P_{W_1}\right)^2 z_1^{[0,1],[0,0]} z_2^{F_{1,1}[1],F_{2,2}[1]} + \\
&\left(P_{G_{1,2}}\right)\left(P_{G_{2,1}}\right)\left(P_{W_1}\right)\left(P_{W_2}\right) z_1^{[0,0],[0,0]} z_2^{F_{1,1}[1],F_{2,2}[0]} + \left(P_{G_{1,2}}\right)\left(P_{G_{2,1}}\right)\left(P_{W_1}\right)^2 z_1^{[0,0],[0,1]} z_2^{F_{1,1}[1],F_{2,2}[0]} + \\
&\left(P_{G_{1,1}}\right)\left(P_{G_{2,2}}\right)\left(P_{W_2}\right)^2 z_1^{[0,2],[1,0]} z_2^{F_{1,1}[0],F_{2,2}[1]} + \left(P_{G_{1,1}}\right)\left(P_{G_{2,2}}\right)\left(P_{W_1}\right)\left(P_{W_2}\right) z_1^{[0,1],[1,0]} z_2^{F_{1,1}[0],F_{2,2}[1]} + \\
&\left(P_{G_{1,1}}\right)\left(P_{G_{2,1}}\right)\left(P_{W_2}\right)^2 z_1^{[0,0],[1,0]} z_2^{F_{1,1}[0],F_{2,2}[0]} + \left(P_{G_{1,1}}\right)\left(P_{G_{2,1}}\right)\left(P_{W_1}\right)\left(P_{W_2}\right) z_1^{[0,0],[1,1]} z_2^{F_{1,1}[0],F_{2,2}[0]} + \\
&\left(P_{G_{1,1}}\right)\left(P_{G_{2,2}}\right)\left(P_{W_1}\right)\left(P_{W_2}\right) z_1^{[0,2],[2,0]} z_2^{F_{1,1}[0],F_{2,2}[1]} + \left(P_{G_{1,1}}\right)\left(P_{G_{2,2}}\right)\left(P_{W_1}\right)^2 z_1^{[0,1],[2,0]} z_2^{F_{1,1}[0],F_{2,2}[1]} + \\
&\left(P_{G_{1,1}}\right)\left(P_{G_{2,1}}\right)\left(P_{W_1}\right)\left(P_{W_2}\right) z_1^{[0,0],[2,0]} z_2^{F_{1,1}[0],F_{2,2}[0]} + \left(P_{G_{1,1}}\right)\left(P_{G_{2,1}}\right)\left(P_{W_1}\right)^2 z_1^{[0,0],[2,1]} z_2^{F_{1,1}[0],F_{2,2}[0]}
\end{aligned}
$$

$+P_{G_{1,2}}P_{W_1} z_1^{[0,0]} z_2^{F_{1,1}[1]} + P_{G_{1,1}}P_{W_2} z_1^{[0,1]} z_2^{F_{1,1}[0]} + P_{G_{1,1}}P_{W_1} z_1^{[0,2]} z_2^{F_{1,1}[0]}$

GPU II: $\Delta_2(z_1,z_2) = u_2(z_1,z_2) \underset{\Leftrightarrow}{\otimes} \omega_2(z_1,z_2)$

(4) The UGF of the performance deficiency vector $\widetilde{D}$ under performance sharing is

$$
\begin{aligned}
&\widetilde{U}_A(z_1,z_2) = U_\Omega(z_1,z_2) \odot \eta(z_1) \\
&= \left(\left(P_{G_{1,3}}\right)\left(P_{G_{2,2}}\right) + \left(P_{G_{1,2}}\right)\left(P_{G_{2,2}}\right)\right) z_1^{[0,0]} z_2^{F_{1,1}[1],F_{2,2}[1]} + \left(\left(P_{G_{1,3}} + P_{G_{1,2}}\right)P_{G_{2,1}}P_{W_2} + \left(P_{G_{1,3}} + P_{G_{1,2}}P_{W_2}\right)P_{G_{2,1}}P_{W_1}\left(P_{C_3} + P_{C_2}\right)\right) z_1^{[0,0]} z_2^{F_{1,1}[1],F_{2,2}[0]} \\
&+P_{G_{1,1}}P_{G_{2,2}}P_{W_2}\left(\left(P_{C_3} + P_{C_2}\right) + P_{W_1}P_{C_3}\right) z_1^{[0,0]} z_2^{F_{1,1}[0],F_{2,2}[1]} + \left(P_{G_{2,1}}P_{W_1}\left(P_{G_{1,3}}P_{C_1} + P_{G_{1,2}}\left(P_{W_1} + P_{W_2}P_{C_1}\right)\right)\right) z_1^{[0,1]} z_2^{F_{1,1}[1],F_{2,2}[0]} + \\
&P_{G_{1,1}}P_{G_{2,2}}P_{W_1}P_{C_1} z_1^{[2,0]} z_2^{F_{1,1}[0],F_{2,2}[1]} + P_{G_{1,1}}P_{G_{2,2}}\left(P_{W_2}P_{C_1} + P_{W_1}\left(P_{W_2}P_{C_2} + P_{W_1}\left(P_{C_3} + P_{C_2}\right)\right)\right) z_1^{[1,0]} z_2^{F_{1,1}[0],F_{2,2}[1]} + \\
&\left(P_{G_{1,1}}\right)\left(P_{G_{2,1}}\right)\left(P_{W_2}\right)^2 z_1^{[1,0]} z_2^{F_{1,1}[0],F_{2,2}[0]} + \left(P_{G_{1,1}}\right)\left(P_{G_{2,1}}\right)\left(P_{W_1}\right)\left(P_{W_2}\right) z_1^{[1,1]} z_2^{F_{1,1}[0],F_{2,2}[0]} + \\
&\left(P_{G_{1,1}}\right)\left(P_{G_{2,1}}\right)\left(P_{W_1}\right)\left(P_{W_2}\right) z_1^{[2,0]} z_2^{F_{1,1}[0],F_{2,2}[0]} + \left(P_{G_{1,1}}\right)\left(P_{G_{2,1}}\right)\left(P_{W_1}\right)^2 z_1^{[2,1]} z_2^{F_{1,1}[0],F_{2,2}[0]}
\end{aligned}
$$

$= P_{G_{2,2}}P_{W_2} z_1^{[2,0]} z_2^{F_{2,2}[1]} + P_{G_{2,2}}P_{W_1} z_1^{[1,0]} z_2^{F_{2,2}[1]} +$

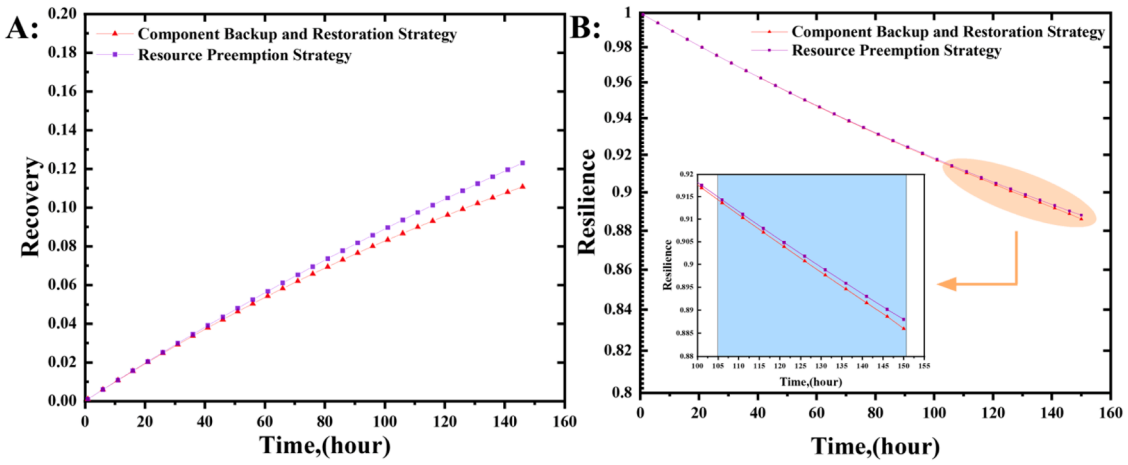

Fig. 8. Trend of recovery resilience and system resilience under different dynamic reconfiguration strategies in the case of system degradation.

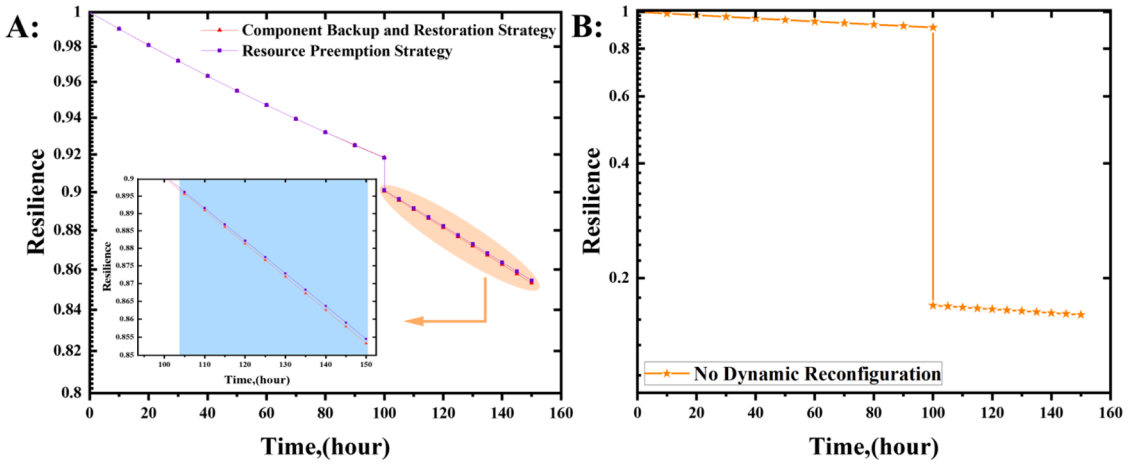

Fig. 9. The trend of system resilience under different dynamic reconfiguration strategies in the case of system failure.

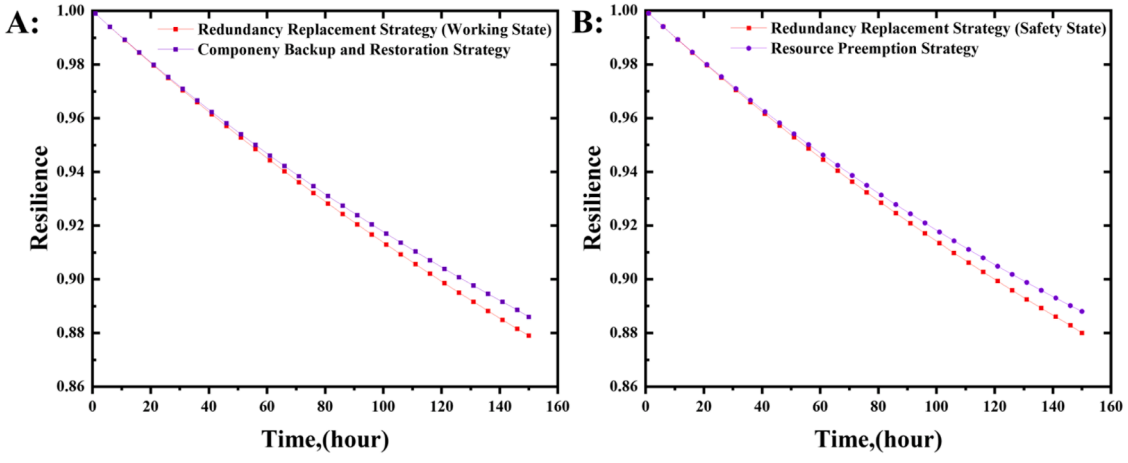

Fig. 10. The trend of system resilience under different dynamic reconfiguration strategies and redundancy replacement strategy.

(5) Resistance resilience$\Re_d$and response resilience$\Re_x$can be described as

$$\Re_d = \left(P_{G_{1,3}}\right)\left(P_{G_{2,2}}\right) + \left(P_{G_{1,2}}\right)\left(P_{G_{2,2}}\right)$$
$$\Re_x = P_{G_{1,3}}P_{G_{2,1}}P_{W_2} + P_{G_{1,3}}P_{G_{2,1}}P_{W_1}\left(P_{C_3} + P_{C_2}\right) + P_{G_{1,2}}P_{G_{2,1}}P_{W_2} + P_{G_{1,2}}P_{G_{2,1}}P_{W_1}P_{W_2}\left(P_{C_3} + P_{C_2}\right) + P_{G_{1,1}}P_{G_{2,2}}P_{W_2}\left(P_{C_3} + P_{C_2}\right) + P_{G_{1,1}}P_{G_{2,2}}P_{W_1}P_{W_2}P_{C_3}$$

(6) Recovery resilience$\Re_{h_1}$under the component backup and recovery strategy is

$$\Re_{h_1} = \left(P_{G_{1,3}} + P_{G_{1,2}}\right)P_{G_{1,3}}P_{G_{2,1}}P_{W_2} + \left(P_{G_{1,3}} + P_{G_{1,2}}\right)P_{G_{1,3}}P_{G_{2,1}}P_{W_1}\left(P_{C_3} + P_{C_2}\right) + \left(P_{G_{1,3}} + P_{G_{1,2}}\right)P_{G_{1,2}}P_{G_{2,1}}P_{W_1}\left(P_{C_3} + P_{C_2}\right) + P_{G_{1,3}}P_{G_{1,2}}P_{G_{2,1}}P_{W_2} + P_{G_{1,2}}{}^2P_{G_{2,1}}P_{W_2} + P_{G_{1,2}}P_{G_{1,1}}P_{G_{2,1}}P_{W_2}{}^2 + \left(P_{G_{1,3}} + P_{G_{1,2}}\right)\left(P_{G_{1,1}}P_{G_{2,2}}P_{W_2}\left(P_{C_3} + P_{C_2}\right)\right) + \left(P_{G_{1,3}} + P_{G_{1,2}}\right)P_{G_{1,1}}P_{G_{2,2}}P_{W_1}P_{C_3}$$

(7) Recovery resilience$\Re_{h_2}$under the resource preemption strategy is

$$\Re_{h_2} = P_{G_{1,3}} + P_{G_{1,2}} + \left(P_{C_3} + P_{C_2}\right)P_{G_{1,1}}P_{G_{2,2}}P_{W_2} + P_{C_3}P_{G_{2,2}}P_{G_{1,1}}P_{W_1} - \Re_d$$

(8) Simulation analysis of system resilience under two dynamic reconfiguration strategies.

a. The trend of system resilience of GPUs considering degradation

Fig. 8 shows the trend of system resilience when only the degradation is considered. The trends of system recovery resilience under two recovery strategies are shown in Fig. 8A. The recovery resilience gradually increases over time, and the rate of increase slows down. The system has greater recovery resilience under the resource preemption strategy than under the component backup and recovery strategy.

The trends of system resilience under two recovery strategies are shown in Fig. 8B. The system resilience gradually decreases with time when only the degradation is considered. When$t = 150h$, the system resilience is 0.886 under the component backup and recovery strategy and 0.888 under the resource preemption strategy. The system resilience is marginally greater and the rate of decline is slightly slower under the resource preemption strategy than under the component backup and recovery strategy.

b. The trend of system resilience of GPUs considering failure

When the GPU I in the system ceases to function due to a failure occurred when$t = 100h$during a mission, the trend of system resilience is shown in Fig. 9. As the diagram indicates, when GPU I fails to work, the system resilience rapidly declines: it decreases by 0.0179 for the component backup and recovery strategy and 0.0172 for the resource preemption strategy. Without any dynamic reconfiguration mechanisms, the resilience drops by 0.7407. The results show that dynamic reconfiguration mechanisms can effectively restore system resilience. Under the same condition, compared to the component backup and recovery strategy, the resource preemption strategy brings a slower decline in system resilience and a better resilience recovery effect when the system fails.

In conclusion, when a sudden failure occurs, the resilience recovery under the component backup and recovery strategy is slightly less than that under the resource preemption strategy. However, instead of simply focusing on the number, it should be noted that the two strategies have different aims: the component backup and recovery strategy focuses on maintaining the normal operation of the system (working state). While the resource preemption strategy emphasizes ensuring the safety of system operations (safe state). Therefore, the choice of dynamic reconfiguration strategy should be based on the usage scenario and objectives.

c. Comparative analysis of results

The redundancy replacement strategy is widely used in the integrated task processing system of the IMA. The strategy is to use spare GPUs to replace the disrupted GPUs [44]. To evaluate the effectiveness

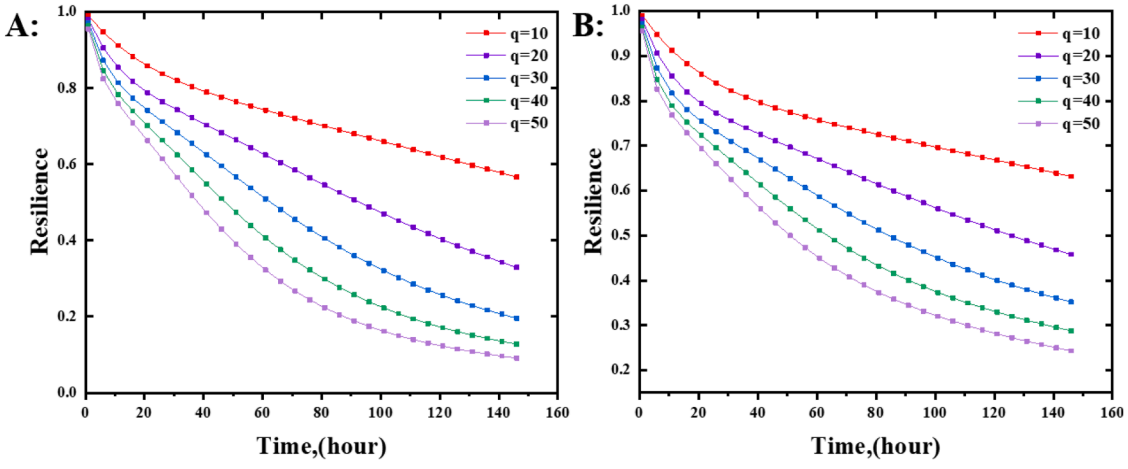

Fig. 11. The trend of system resilience under different dynamic reconfiguration strategies in different intensity of random disturbances.

of the proposed method, the trend of system resilience is shown in Fig. 10. Fig. 10A indicates that when strategies focus on maintaining the working state of the system and$t = 150h$, the system resilience is 0.886 under the component backup and recovery strategy and 0.879 under the redundancy replacement strategy. Although the operation mechanism of the redundancy replacement strategy is similar to that of the component backup and recovery strategy, the former does not consider the performance sharing mechanism due to the assumed independence between units [44]. The result suggests that the dependencies between units, such as the performance sharing mechanism, significantly influence the resilience assessment results. Under identical conditions, the results are higher when performance sharing is considered than when it is overlooked.

In addition, Fig. 10B indicates that when strategies focus on ensuring the system is safe and$t = 150h$, the system resilience is 0.888 under the resource preemption strategy and 0.880 under the redundancy replacement strategy. Furthermore, the results indicate that dynamic reconfiguration strategies achieve slightly higher system resilience and exhibit a slower decline rate compared to the redundancy replacement strategy proposed in [44]. The result indicates that under identical conditions, the proposed resource preemption strategy is more effective in enhancing system resilience than the redundancy replacement.

In conclusion, the results indicate the critical importance of considering dependencies between units by incorporating these dependencies, mainly through performance sharing mechanisms, the accuracy of resilience evaluations is enhanced, which in turn better demonstrates the effectiveness of dynamic reconfiguration strategies in improving system resilience.

d. Sensitivity analysis

The impact of random disturbances on system resilience is studied to analyze the sensitivity of the proposed model. When the random disturbances accelerate the degradation rate ($\lambda' = q\lambda$), the trend of system resilience is shown in Fig. 11. Fig. 11 A indicates the trend of system resilience under component backup and restoration strategy, and Fig. 11 B indicates the trend of system resilience under resource preemption strategy. As the diagram suggests, the rate of decline dramatically increases over time with the increasing intensity of random disturbances. Moreover, the sensitivity gradually decreases when the intensity of random disturbances increases. The system under the component backup and restoration strategy is more sensitive than the resource preemption strategy.

5. Conclusion

Due to the lack of resilience modeling and evaluation methods suitable for multi-state system with common bus performance sharing (MSS-CBPS) under dynamic reconfiguration, the paper presents a novel resilience assessment framework for MSS-CBPS under dynamic reconfiguration. The proposed model comprehensively considers dynamic reconfiguration and the sequence of performance allocation, evaluating system resilience from three aspects: resistance, response, and recovery. Additionally, combining UGF with the proposed resilience model, this paper proposes an algorithm for evaluating the resilience of MSS-CBPS under two different dynamic reconfiguration strategies, effectively addressing the challenges in quantitatively evaluating the resilience of MSS-CBPS.

A case study of an integrated task processing system in the helicopter is conducted to demonstrate the feasibility of the proposed resilience model and evaluation method and to support the resilience design of the system. The results show that, as system degradation occurs, system resilience gradually declines over time; when using the component backup and recovery strategy, the system's resilience is 0.886; for the resource preemptive strategy, the system's resilience is 0.888. Compared to the component backup and recovery strategy, the system exhibits greater resilience and a slower decline rate of resilience under the resource preemption strategy. When a failure occurs in the system, the system's resilience quickly decreases; under the component backup and recovery strategy, the resilience decreases by 0.0179; under the resource preemption strategy, it decreases by 0.0172; and without any dynamic reconfiguration strategies, it decreases by 0.7407. The results show that the dynamic reconfiguration strategies can effectively enhance the system's ability to handle failures. Furthermore, the resilience under the resource preemption strategy declines more slowly and shows better recovery in the case of system failure. It should be noted, however, that two strategies have different focuses and a choice between them needs to be based on the scenario and aim. Additionally, a comparative analysis and sensitivity analysis is also studied to assess the feasibility of the proposed resilience model and evaluation method.

However, this study is not without its limitations. First, it only focuses on two dynamic reconfiguration strategies: component backup and recovery and resource preemption. Future work could consider incorporating additional dynamic reconfiguration strategies to address various failure scenarios. Second, the model faces the challenge of state explosion problems in multi-state systems. Developing more efficient algorithms to address the issue may enhance the model processing capability and efficiency. Finally, exploring the optimization of system composition structures presents an important way to improve resilience in the face of different failures.

CRediT authorship contribution statement

Gengshuo Hu: Writing – original draft, Methodology, Formal analysis. **Xing Pan:** Writing – review & editing. **Jian Jiao:** Writing – review & editing, Methodology.

Declaration of competing interest

The authors declare that they have no known competing financial interests or personal relationships that could have appeared to influence the work reported in this paper.

Appendix

Nomenclature

$G_i(t)$	random performance
$W_i(t)$	random performance demand
$C(t)$	transmission capacity
n	the number of components in the system
n_1	the number of major components
$\alpha_i(t)$	the probabilities of units or bus in every state
Q_i	State transition probability density matrix
$S_i(t)$	performance surplus of $unit_i$
$D_i(t)$	performance deficiency of $unit_i$
$\Re_x$	response resilience
$\Re_h$	recovery resilience
$\Re_{h_1}$	recovery resilience under the component backup and recovery strategy
$\Re_{h_2}$	recovery resilience under the resource preemption strategy
$\Re_{system}$	system resilience
$u_i(z_1, z_2)$	the UGF presenting the pmf of$G_i(t)$
$\omega_i(z_1, z_2)$	the UGF presenting the pmf of$W_i(t)$
F	the vector of operation state
F_{j_h}	the vector of operation state under the component backup and recovery strategy

(*continued on next page*)

(*continued*)

S	the vector of performance surplus	F_{j_e}	the vector of operation state under the resource preemption strategy
D	the vector of performance deficiency	$\Delta_i(z_1, z_2)$	UGF presenting the combined pmf S_i, D_i and F_i
$T(t)$	redistributed performance surplus	$U_\Omega(z_1, z_2)$	UGF presenting the combined pmf S, D and F
$\widetilde{D}$	the vector of performance deficiency under performance sharing	$\eta(z_1)$	UGF presenting the pmf of $C(t)$
$\overline{D}$	the vector of performance deficiency under the component backup and recovery strategy	$\widetilde{U}_A(z_1, z_2)$	UGF presenting the combined pmf $\widetilde{D}$ and F
$\widehat{D}$	the vector of performance deficiency under the resource preemption strategy	$\overline{U}_B(z_1, z_2)$	UGF presenting the combined pmf $\overline{D}$ and F_{j_b}
N_1	the number of major units in a working state	$\widehat{U}_E(z_1, z_2)$	UGF presenting the combined pmf $\widehat{D}$ and F_{j_e}
N_2	the number of minor units in a working state		
$\overline{n}_1$	specified number of major units		
$\overline{n}_2$	specified number of minor units		
$\Re_d$	resistance resilience		

References

[1] Qiu S, Ming HXG. Reliability evaluation of multi-state series-parallel systems with common bus performance sharing considering transmission loss [J]. Reliab Eng Syst Saf 2019;189:406–15. https://doi.org/10.1016/j.ress.2019.04.029.

[2] Li YF, Peng R. Availability modeling and optimization of dynamic multi-state series–parallel systems with random reconfiguration [J]. Reliab Eng Syst Saf 2014; 127:47–57. https://doi.org/10.1016/j.ress.2014.03.005.

[3] Su P, Wang G, Duan F. Reliability analysis for k-out-of-(n+ 1): g star configuration multi-state systems with performance sharing [J]. Comput Ind Eng 2021;152: 106991. https://doi.org/10.1016/j.cie.2020.106991.

[4] Xiao H, Peng R. Optimal allocation and maintenance of multi-state elements in series–parallel systems with common bus performance sharing [J]. Comput Ind Eng 2014;72:143–51. https://doi.org/10.1016/j.cie.2014.03.014.

[5] Cheng Y, Elsayed EA, Huang Z. Systems resilience assessments: a review, framework and metrics [J]. Int J Prod Res 2022;60(2):595–622. https://doi.org/10.1080/00207543.2021.1971789.

[6] Lisnianski A, Ding Y. Redundancy analysis for repairable multi-state system by using combined stochastic processes methods and universal generating function technique [J]. Reliab Eng Syst Saf 2009;94(11):1788–95. https://doi.org/10.1016/j.ress.2009.05.006.

[7] Levitin G. Reliability of multi-state systems with common bus performance sharing [J]. IIE Trans 2011;43(7):518–24. https://doi.org/10.1080/0740817X.2010.523770.

[8] Zhao X, Wu C, Wang S, et al. Reliability analysis of multi-state k-out-of-n: g system with common bus performance sharing [J]. Comput Ind Eng 2018;124:359–69. https://doi.org/10.1016/j.cie.2018.07.034.

[9] Su P, Wang G, Duan F. Reliability evaluation of a k-out-of-n (G)-subsystem based multi-state system with common bus performance sharing [J]. Reliab Eng Syst Saf 2020;198:106884. https://doi.org/10.1016/j.ress.2020.106884.

[10] Xiao H, Zhang Y, Xiang Y, et al. Optimal design of a linear sliding window system with consideration of performance sharing [J]. Reliab Eng Syst Saf 2020;198: 106900. https://doi.org/10.1016/j.ress.2020.106900.

[11] Peng R. Optimal component allocation in a multi-state system with hierarchical performance sharing groups [J]. J Operat Res Soc 2019;70(4):581–7. https://doi.org/10.1080/01605682.2018.1448697.

[12] Peng R, Liu H, Xie M. A study of reliability of multi-state systems with two performance sharing groups [J]. Qual Reliab Eng Int 2016;32(7):2623–32. https://doi.org/10.1002/qre.1963.

[13] Wu C, Pan R, Zhao X, et al. Reliability evaluation of consecutive-k-out-of-n: f systems with two performance sharing groups [J]. Comput Ind Eng 2021;153: 107092. https://doi.org/10.1016/j.cie.2020.107092.

[14] Gu L, Wang G, Zhou Y, et al. Reliability optimization of multi-state systems with two performance sharing groups [J]. Reliab Eng Syst Saf 2024;241:109580. https://doi.org/10.1016/j.ress.2023.109580.

[15] Yu H, Yang J, Zhao Y. Reliability of nonrepairable phased-mission systems with common bus performance sharing [J]. Proc Inst Mech Eng Part O: J Risk Reliab 2018;232(6):647–60. https://doi.org/10.1177/1748006X18757074.

[16] Cheng C, Yang J, Li L. Reliability assessment of multi-state phased mission systems with common bus performance sharing considering transmission loss and performance storage [J]. Reliab Eng Syst Saf 2020;199:106917. https://doi.org/10.1016/j.ress.2020.106917.

[17] Cheng C, Yang J, Li L. Reliability assessment of multi-state phased mission systems with common bus performance sharing subjected to epistemic uncertainty [J]. IEEE Trans Reliab 2021;71(3):1281–93. https://doi.org/10.1109/TR.2021.3077486.

[18] Qiu S, Ming X. A fuzzy universal generating function-based method for the reliability evaluation of series systems with performance sharing between adjacent units under parametric uncertainty [J]. Fuzzy Sets Syst 2021;424:155–69. https://doi.org/10.1016/j.fss.2020.08.013.

[19] Wu C, Pan R, Zhao X, et al. Designing preventive maintenance for multi-state systems with performance sharing [J]. Reliab Eng Syst Saf 2024;241:109661. https://doi.org/10.1016/j.ress.2023.109661.

[20] Si S, Levitin G, Dui H, et al. Importance analysis for reconfigurable systems [J]. Reliab Eng Syst Saf 2014;126:72–80. https://doi.org/10.1016/j.ress.2014.01.012.

[21] Li YF, Peng R. Availability modeling and optimization of dynamic multi-state series–parallel systems with random reconfiguration [J]. Reliab Eng Syst Saf 2014; 127:47–57. https://doi.org/10.1016/j.ress.2014.03.005.

[22] Zhai Q, Ye ZS, Peng R, et al. Defense and attack of performance-sharing common bus systems [J]. Eur J Operat Res 2017;256(3):962–75. https://doi.org/10.1016/j.ejor.2016.06.059.

[23] Levitin G, Xing L, Huang HZ. Dynamic availability and performance deficiency of common bus systems with imperfectly repairable components [J]. Reliab Eng Syst Saf 2019;189:58–66. https://doi.org/10.1016/j.ress.2019.04.007.

[24] Dessavre DG, Ramirez-Marquez JE, Barker K. Multidimensional approach to complex system resilience analysis [J]. Reliab Eng Syst Saf 2016;149:34–43. https://doi.org/10.1016/j.ress.2015.12.009.

[25] Alhozaimy S, Menascé DA, Albanese M. Resilience and performance quantification of dynamic reconfiguration [J]. Future Generat Comput Syst 2024. https://doi.org/10.1016/j.future.2024.05.040.

[26] Zeng Z, Fang YP, Zhai Q, et al. A Markov reward process-based framework for resilience analysis of multistate energy systems under the threat of extreme events [J]. Reliab Eng Syst Saf 2021;209:107443. https://doi.org/10.1016/j.ress.2021.107443.

[27] Tan Z, Wu B, Che A. Resilience modeling for multi-state systems based on Markov processes [J]. Reliab Eng Syst Saf 2023;235:109207. https://doi.org/10.1016/j.ress.2023.109207.

[28] Dui H, Lu Y, Wu S. Competing risks-based resilience approach for multi-state systems under multiple shocks [J]. Reliab Eng Syst Saf 2024;242:109773. https://doi.org/10.1016/j.ress.2023.109773.

[29] Wang JW, Gao F, Ip WH. Measurement of resilience and its application to enterprise information systems [J]. Enterp Inf Syst 2010;4(2):215–23. https://doi.org/10.1080/17517571003754561.

[30] Luo MY, Yang CS. Enabling fault resilience for web services [J]. Comput Commun 2002;25(3):198–209. https://doi.org/10.1016/S0140-3664(01)00363-2.

[31] Todman LC, Fraser FC, Corstanje R, et al. Defining and quantifying the resilience of responses to disturbance: a conceptual and modelling approach from soil science [J]. Sci Rep 2016;6(1):28426.

[32] He L, Wu Z, Xiang W, et al. A novel Kano-QFD-DEMATEL approach to optimise the risk resilience solution for sustainable supply chain [J]. Int J Prod Res 2021;59(6): 1714–35.

[33] Rose A. Economic resilience to natural and man-made disasters: multidisciplinary origins and contextual dimensions [J]. Environl Hazards 2007;7(4):383–98. https://doi.org/10.1016/j.envhaz.2007.10.001.

[34] Gao Y, Wang JW. A resilience assessment framework for urban transportation systems [J]. Int J Prod Res 2021;59(7):2177–92.

[35] Giahi R, MacKenzie CA, Hu C. Design optimization for resilience for risk-averse firms [J]. Comput Ind Eng 2020;139:106122. https://doi.org/10.1016/j.cie.2019.106122.

[36] Toroghi SSH, Thomas VM. A framework for the resilience analysis of electric infrastructure systems including temporary generation systems [J]. Reliab Eng Syst Saf 2020;202:107013. https://doi.org/10.1016/j.ress.2020.107013.

[37] Bruneau M, Chang SE, Eguchi RT, et al. A framework to quantitatively assess and enhance the seismic resilience of communities [J]. Earthquake Spectra 2003;19(4): 733–52.

[38] Zhao J, Lee JY, Camenzind D, et al. Multi-component resilience assessment framework for a supply chain system [J]. Sustainability 2023;15(7):6197. https://doi.org/10.3390/su15076197.

[39] Chen Z, Hong D, Cui W, et al. Resilience assessment and Optimal Design for Weapon System of Systems with Dynamic Reconfiguration [J]. Reliab Eng Syst Saf 2023:109409. https://doi.org/10.1016/j.ress.2023.109409.

[40] Pan X, Dang Y, Wang H, et al. Resilience model and recovery strategy of transportation network based on travel OD-grid analysis [J]. Reliab Eng Syst Saf 2022;223:108483. https://doi.org/10.1016/j.ress.2022.108483.

[41] Yarveisy R, Gao C, Khan F. A simple yet robust resilience assessment metrics [J]. Reliab Eng Syst Saf 2020;197:106810. https://doi.org/10.1016/j.ress.2020.106810.

[42] Ren F, Zhao T, Jiao J, et al. Resilience optimization for complex engineered systems based on the multi-dimensional resilience concept [J]. IEEE Access 2017;5: 19352–62. https://doi.org/10.1109/ACCESS.2017.2755043.
[43] Levitin G. The universal generating function in reliability analysis and optimization [M]. London: Springer; 2005.
[44] Chu J, Zhao T, Jiao J, et al. Optimal design of configuration scheme for integrated modular avionics systems with functional redundancy requirements [J]. IEEE Syst J 2020;15(2):2665–76. https://doi.org/10.1109/JSYST.2020.2993636.